

Microstructure and Properties of $\text{La}_{0.7}\text{Sr}_{0.3}\text{MnO}_3$ Films Deposited on LaAlO_3 (100), (110), and (111) Substrates

Du Yongsheng (杜永胜)¹, Zhang Xuefeng (张雪峰)^{1*}, Yu Dunbo (于敦波)², Yan Hui (严辉)³

(1. College of Science, Inner Mongolia University of Science & Technology, Baotou 014010, China; 2. Girem Advanced Materials Co., Ltd., Beijing 100088, China; 3. Laboratory of Thin Film Materials, Beijing University of Technology, Beijing 100022, China)

Received 30 December 2005; revised 5 June 2006

Abstract: A comparative study of the crystalline structure, magnetic properties, and transport properties of LSMO films grown on (100)-, (110)-, and (111) LaAlO_3 (LAO) substrates was carried out. Using atomic force microscopy, round, rectangle, and dot surface morphologies were observed in (100)-, (110)-, and (111)-oriented LSMO films, respectively. Electrical and magnetic characterizations were performed on LSMO films of different orientation to provide evidence for the effect of strain on the magnetotransport properties. The (111)-oriented LSMO film has higher saturation magnetization and lower resistance compared with the (100)- and (110)-oriented LSMO films, which results from the smaller elastic deformation due to the larger elastic modulus along the $\langle 111 \rangle$ crystallographic direction.

Key words: $\text{La}_{0.7}\text{Sr}_{0.3}\text{MnO}_3$ film; strain; crystallographic; elastic modulus; rare earths

CLC number: O469 **Document code:** A **Article ID:** 1002-0721(2006)05-0560-04

Recently, doped perovskite manganite has kindled a renewed interest because they exhibit a variety of unique magnetic and electronic behaviors such as colossal magnetoresistance (CMR), percolative phase separation, and spin/charge/orbital ordering^[1–3]. The emphasis of both theoretical and experimental studies of doped materials has been the effect of CMR because it can be used for potential application in magnetic devices. As a member of the CMR materials, $\text{La}_{0.7}\text{Sr}_{0.3}\text{MnO}_3$ (LSMO) possesses the highest values of Curie temperature (> 370 K), which makes it a very promising material in room-temperature applications.

However, the origin of CMR in LSMO films is still not clear although it has been the focus of several stud-

ies. As is well known, the magnetic and transport properties of LSMO films are closely associated with strain and it is very important to understand the role played by strain in deciding the properties of LSMO films^[4–7]. The effect of strain on the properties of films has been studied only in ($h00$) LSMO films and the possible influence of the strain on the properties of ($hh0$) and (hhh) films remains obscure^[4,8]. The elastic modulus of different LSMO films varies with the orientation of the film, which can result in different strains. To solve these problems, we deposited LSMO films on (100), (110), and (111) LAO substrates using the RF magnetron sputtering technique and studied the effects of strain on the properties of LSMO films.

* Corresponding author (E-mail: xuefeng056@163.com)

Foundation item: Project supported by the Key Basic Research Project of MOST (2002CCC01300), the Natural Science Foundation of Beijing (2021003), and the Science & Technology Development Project of Beijing Education Committee and Beijing Specific Project to Foster Elitist (20041D0501513)

Biography: Du Yongsheng (1977–), Male, Master

1 Experimental

LSMO films of about 100 nm were deposited on (100), (110), and (111) LAO substrates by RF magnetron sputtering. During the deposition step, the substrates were heated to 800 °C and reactive plasma Ar (80%): O₂(20%) at 1 Pa was used. To improve the oxygen content, the samples were annealed ex situ at 800 °C in flowing oxygen at atmospheric pressure for 0.5 h.

The thickness of the LSMO films was measured using a Seimitzu Surfcom 480A profiler. The XRD diffraction curves of the films were measured using a Bruker diffractometer (AXS D8ADVANCE) with the Cu K α radiation. For all the LSMO films used in this study, the crystallographic planes and their directions are indexed according to cubic notation. The surface morphology of the films was observed using a Digital Nanoscope III atomic force microscopy (AFM). Both the magnetic properties and the electric transport measurements were studied using a physical properties measurement system (PPMS-7) with a standard four probe.

2 Results and Discussion

The X-ray diffraction curves of LSMO films deposited on (100), (110), and (111) LAO substrates are shown in Fig. 1. The result shows that the deposited LSMO films are in epitaxial growth because only those diffraction peaks appear in accordance with the orientation of the substrates. The out-of-plane lattice parameters of (100)-, (110)-, and (111)-oriented LSMO films derived from the XRD results are about 0.393, 0.276, and 0.223 nm, respectively, but the corresponding ideal values of LSMO bulk are 0.388, 0.274, and 0.224 nm, respectively. According to the definition of the out-of-plane strain, $\epsilon_{001} = (c_{\text{film}} - c_{\text{bulk}})/c_{\text{bulk}} \times 100\%$, the out-of-plane strain for (100)-, (110)-, and (111)-oriented LSMO films are about 1.3%, 1.1%, and -0.4%, respectively. The calculated data show that the out-of-plane strain is smaller in the (111)-oriented film compared with the (100)- and (110)-oriented films. However, the degree of lattice mismatches is about 2.3% for all the three oriented LSMO films and LAO substrates because both LSMO ($a = 0.388$ nm) and LAO ($a = 0.379$ nm) are cubic perovskite structures. Accordingly, the out-of-plane compressive stress (σ) of the three oriented LSMO films has the same value. Thus, we can attribute the different out-of-plane strain to the different elastic modulus that can be defined as $E = \sigma/\epsilon$. Note that the (111) plane is the close-packed

plane of atoms in cubic perovskite structures and that the maximum elastic modulus is along the $\langle 111 \rangle$ crystallographic direction^[9]. The larger elastic modulus in films can result in smaller elastic deformation under the same stress, so the lattice disorder in (111)-oriented LSMO film is the smallest among the three oriented LSMO films.

AFM was also used to study the morphology of the films and to estimate surface roughness. The roughness of the (100), (110), and (111) LSMO films, determined from AFM measurements (Fig. 2) in a $1 \mu\text{m} \times 1 \mu\text{m}$ scan area, are about 0.602, 0.718, and 0.526 nm, respectively. We have observed that (111)-oriented films are smoother in comparison with (100)- and (110)-oriented films and this can be attributed to the smaller lattice disorder in (111)-oriented films.

Studies on the in-plane crystallographic relations show a different epitaxial nature of distinct orientations giving rise to a distinct degree of in-plane structural coherence. Round, rectangle, and dot surface morphologies were obtained in (100)-, (110)-, and (111)-oriented LSMO films, respectively. Fig. 3 shows the simulated surface morphologies of the (100), (110), and (111) planes of LSMO. It can be seen that the image of the (100) plane is square with in-plane lattice constant of $a = 0.388$ nm; the (110) plane has an oblong surface structure with in-plane lattice constant of $a = 0.388$ nm and $b = 0.549$ nm, and the (111) plane has a triangle surface morphology with in-plane lattice constant of $a = 0.549$ nm. For the (110) LSMO film, the grains are longer along the [100] than the [110] in-plane direction. As the (100) plane face is more densely packed than the (110) face, it is reasonable that [100] is the direction of faster growth^[10]. This trend is also consistent with AFM images of oblong surface structure in (110)

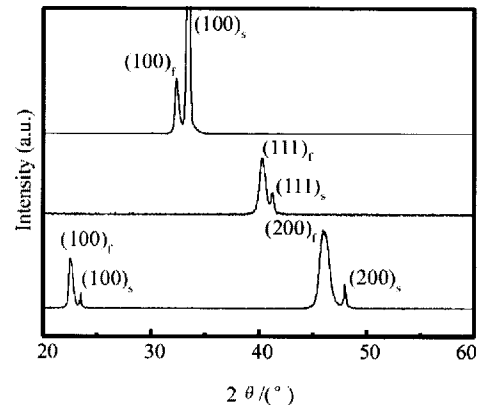


Fig. 1 Diffraction curves for LSMO films deposited on (100), (110), and (111) LAO substrates

films. For the (100)- and (111)-oriented LSMO films, the growth of the (100) and (111) planes along each normal direction has equal values, respectively. As a result, isometric surface morphologies can be found in (100)- and (111)-oriented films.

Fig.4 shows the temperature dependence of magnetization $M(T)$ curves for the LSMO films with an applied field of $79.6 \text{ kA} \cdot \text{m}^{-1}$. It can be seen that the (111)-oriented LSMO film has high saturation magnetization compared with the (100)- and (110)-oriented LSMO films. It is well known that in the LSMO system, there exists a ferromagnetic coupling between Mn^{3+} and Mn^{4+} ions that is caused by the strong

Hund's rule coupling and the spins of two Mn ions being parallel below Curie temperature, which is called the double-exchange interaction^[11]. The strain in (100)- and (110)-oriented LSMO films can produce a

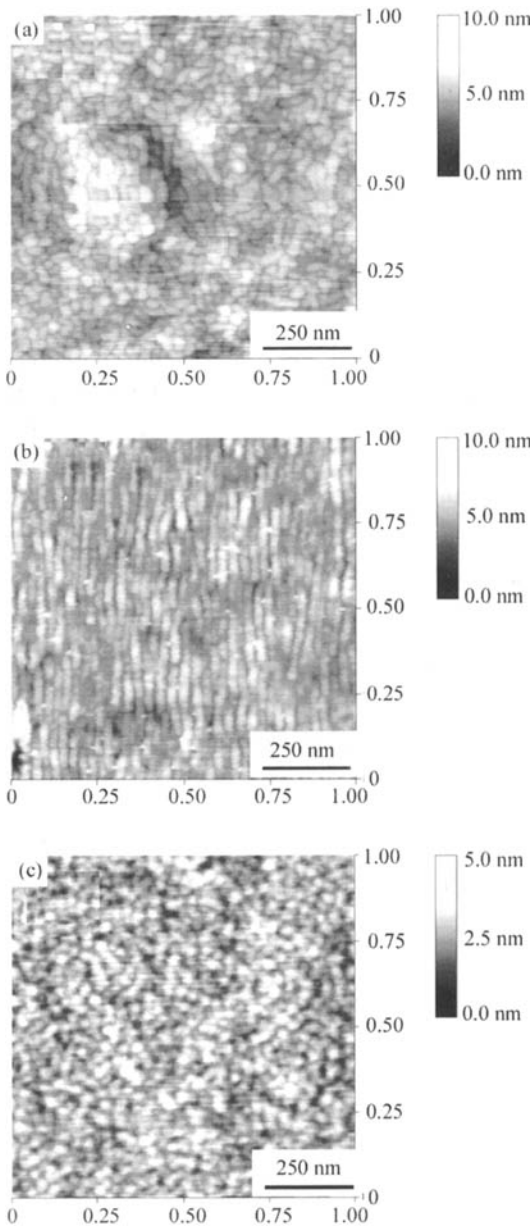


Fig.2 Surface morphology of LSMO epitaxial films deposited on (100), (110), and (111) LAO substrates by AFM (a) (100); (b) (110); (c) (111)

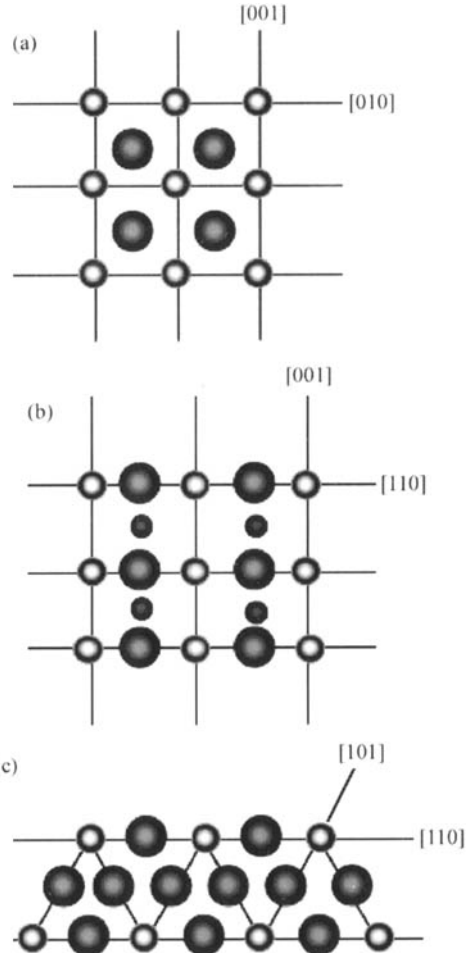


Fig.3 Structural sketch map of LSMO films (a) Top view of structural map of (LaSr)O layer in (100) LSMO film; (b) Top view of structural map of (LaSr)MnO layer in (110) LSMO film; (c) Top view of structural map of (LaSr)O₃ layer in (111) LSMO film

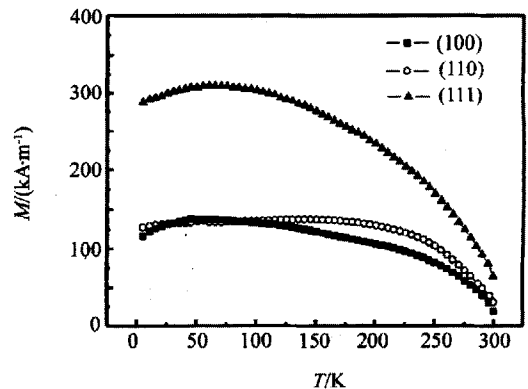


Fig.4 Magnetization $M(H)$ ($T = 5 \text{ K}$) curves for (100), (110), and (111) LSMO films with applied field parallel to the films' plane

large distortion of the $\text{Mn}^{3+}-\text{O}^{2-}-\text{Mn}^{4+}$ bond angles away from 180° , which decreases the ferromagnetic order and reduces the saturation magnetization.

Fig.5 shows the temperature dependence of the resistance for LSMO films at zero field deposited on (100), (110), and (111) LAO substrates, respectively. It was found that the (111)-oriented LSMO film has the lowest resistance among LSMO films of different orientation. It was indicated that the transport properties effect is attributed to the itinerant e_g electrons via $\text{Mn}^{3+}-\text{O}-\text{Mn}^{4+}$, as described with respect to the double-exchange model. The strain can cause a slightly distorted perovskite-type structure, that is, a MnO_6 octahedron is alternately rotated and tilted along the pseudocubic axes, which leads to the change of the Mn-O-Mn bond angle and influences the transport properties^[12]. Parts of the itinerant e_g electrons can be scattered when the Mn-O-Mn bond angle is deviated from 180° ; therefore, the (100)- and (110)-oriented LSMO films have higher resistance values when compared with the value of (111)-oriented film.

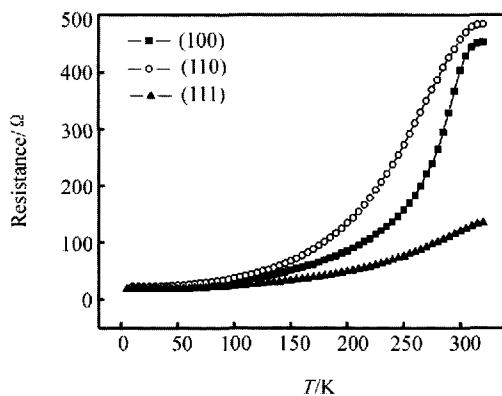


Fig.5 Temperature dependence of resistance for LSMO films at zero field on (100), (110), and (111) LAO substrates

3 Conclusion

In summary, the effect of strain on the magnetic and transport properties in epitaxial LSMO films deposited on (100), (110), and (111) LAO substrates have been investigated. Round, rectangle, and dot surface morphologies were obtained in (100)-, (110)-, and (111)-oriented LSMO films, respectively. The differences in the strain that exist in the (100)-, (110)-, and (111)-oriented LSMO films can result in different magnetic and transport properties.

References:

- [1] Dho Joonghoe, Kim Y N, Hwang Y S, et al. Strain-induced magnetic stripe domains in $\text{La}_{0.7}\text{Sr}_{0.3}\text{MnO}_3$ thin films [J]. Appl. Phys. Lett., 2003, 82: 1434.
- [2] Murakami Y, Yoo J H, Shindo D, et al. Magnetization distribution in the mixed-phase state of hole-doped manganites [J]. Nature, 2003, 423: 965.
- [3] Huang Baoxin, Liu Yihua, Zhang Ruzhen, et al. Spin dependent hopping in Ti doped $\text{La}_{0.67}\text{Ca}_{0.33}\text{MnO}_3$ [J]. Journal of Rare Earths, 2004, 22: 803.
- [4] Fontcuberta J, Bibes M, Martínez B. Epitaxial growth of magnetoresistive (00h), (0hh), and (hhh) $\text{La}_{2/3}\text{Sr}_{1/3}\text{MnO}_3$ thin films on (001)Si substrates [J]. Appl. Phys. Lett., 1999, 74: 1743.
- [5] Nath T K, Rao R A, Lavric D, et al. Effect of three-dimensional strain states on magnetic anisotropy of $\text{La}_{0.8}\text{Ca}_{0.2}\text{MnO}_3$ epitaxial thin films [J]. Appl. Phys. Lett., 1999, 74: 1615.
- [6] Haghiri-Gosnet A M, Wolfman J, Mercey B, et al. Microstructure and magnetic properties of strained $\text{La}_{0.7}\text{Sr}_{0.3}\text{MnO}_3$ thin films [J]. J. Appl. Phys., 2000, 88: 4257.
- [7] Ma Yanwei, Guilloux Viry M, Barahona P, et al. Epitaxial growth of $\text{Gd}_{0.67}\text{Ca}_{0.33}\text{MnO}_3$ thin films by laser ablation [J]. Journal of Rare Earths, 2004, 22: 739.
- [8] Li H Q, Fang Q F, Zhu Z G. Structure and characterization of magnetoresistance of $\text{La}_{0.7}\text{Pb}_{0.3}\text{MnO}_3$ in bulk and films deposited on LaAlO_3 (100), (110) and (111) substrates [J]. Mater. Lett., 2002, 52: 120.
- [9] Doan Trong-Duc, Giocondi Jennifer L, Rohrer Gregory S, et al. Surface engineering along the close-packed direction of SrTiO_3 [J]. J. Cryst. Growth, 2001, 225: 178.
- [10] Berndt L M, Balbarin Vincent, Suzuki Y. Magnetic anisotropy and strain states of (001) and (110) colossal magnetoresistance thin films [J]. Appl. Phys. Lett., 2000, 77: 2903.
- [11] Zener C. Interaction between the d-Shells in the Transition Metals. II. Ferromagnetic Compounds of Manganese with Perovskite Structure [J]. Phys. Rev., 1951, 82: 403.
- [12] Seiro S, Salva H R, Saint-Paul M, et al. Charge ordering and elastic anomalies in $\text{Pr}_{0.65}\text{Ca}_{0.35}\text{MnO}_3$ [J]. J. Phys:Condens. Matter, 2002, 14: 3973.
- [13] Cherif K, Dhahri, Vincent H, et al. X-ray diffraction, magnetic and electrical properties in the manganite $(\text{La}_{1-x}\text{Nd}_x)_{0.7}\text{Sr}_{0.3}\text{MnO}_3$ [J]. Physica B, 2002, 321: 48.
- [14] Zemmi S, Dhahri Ja, Cherif K, et al. The effect of a cation radii on structural, magnetic and electrical properties of doped manganite $\text{La}_{0.6-x}\text{Pr}_x\text{Sr}_{0.4}\text{MnO}_3$ [J]. J Solid State Chem., 2004, 177: 2387.
- [15] Zheng G H, Sun Y P, Zhu X B, et al. Transport, magnetic, internal friction, and Young's modulus in the Y-doped manganite $\text{La}_{0.9-x}\text{Y}_x\text{Te}_{0.1}\text{MnO}_3$ [J]. J Solid State Chem., 2006, 179: 1394.